

# Orientations of the Tryptophan 9 and 11 Side Chains of the Gramicidin Channel Based on Deuterium Nuclear Magnetic Resonance Spectroscopy

Roger E. Koeppe, II,<sup>\*†</sup> J. Antoinette Killian,<sup>‡</sup> and Denise V. Greathouse<sup>\*</sup>

<sup>\*</sup>Department of Chemistry and Biochemistry, University of Arkansas, Fayetteville, Arkansas, USA, and <sup>‡</sup>Department of Biochemistry of Membranes, Center for Biomembranes and Lipid Enzymology, University of Utrecht, Utrecht, the Netherlands

**ABSTRACT** Deuterium nuclear magnetic resonance spectroscopy was used to investigate the orientations of the indole rings of Trp<sup>9</sup> and Trp<sup>11</sup> in specific indole-*d*<sub>5</sub>-labeled samples of gramicidin A incorporated into dimyristoyl phosphatidylcholine bilayers in the  $\beta^{6,3}$  channel conformation. The magnitudes and signs of the deuterium quadrupolar splittings were fit to the rings and assigned to specific ring bonds, using a full rotation search of the  $\chi_1$  and  $\chi_2$  angles of each Trp and a least-squares method. Unique assignments were obtained. The data and assignments are in close agreement with four sets of ( $\chi_1$ ,  $\chi_2$ ) angles for each Trp in which the indole N-H is oriented toward the membrane's exterior surface. (Four additional sets of ( $\chi_1$ ,  $\chi_2$ ) angles with the N-H's pointing toward the membrane interior are inconsistent with previous observations.) One of the sets of ( $\chi_1$ ,  $\chi_2$ ) angles for each Trp is consistent with the corresponding Trp orientation found by Arsen'ev et al. (1986. *Biol. Membr.* 3:1077–1104) for gramicidin in sodium dodecyl sulfate micelles. Together, the <sup>1</sup>H and <sup>2</sup>H nuclear magnetic resonance methods suggest that the Trp<sup>9</sup> and Trp<sup>11</sup> side chain orientations could be very similar in dimyristoyl phosphatidylcholine membranes and in sodium dodecyl sulfate micelles. The data for Trp<sup>11</sup> could be fit using a static quadrupolar coupling constant of 180 kHz under the assumption that the ring is essentially immobile. By contrast, Trp<sup>9</sup> could be fit only under the assumption that the quadrupolar splittings for ring 9 are reduced by approximately 14% due to motional averaging. Such a difference in motional averaging between rings 11 and 9 is also consistent with the <sup>15</sup>N data of Hu et al. (1993. *Biochemistry.* 32:7035–7047).

## INTRODUCTION

The gramicidin A (gA) channel is formed by hydrogen bonding at the formyl-NH-termini of two gA monomers, each spanning half of the membrane, with the entrance being formed by the COOH-terminal ends of the polypeptide backbone of the respective monomers (Urry, 1971; Andersen and Koeppe, 1992; Killian, 1992). The tryptophan residues at positions 9, 11, 13, and 15 of the gA sequence (Sarges and Witkop, 1965) are situated near the membrane-water interface, where they approximately surround the channel entrance. These residues are important for the structure and function of the peptide as well as its interaction with lipids. The Trp residues play a role in the folding of gA into the dimeric  $\beta^{6,3}$  channel conformation (Urry, 1971; Koeppe et al., 1992; Durkin et al., 1992) in bilayers (Sawyer et al., 1990); they also affect channel conductance and stability (Becker et al., 1991), and they are essential for the modulation of lipid structure by incorporated gA (Killian, 1992).

Being at the periphery of the gA molecule, the Trp indole rings are in positions to interact with the surrounding molecules as they perform their various functions. Critical to such function are the precise orientations and motions of each

indole ring within the gA/lipid complex. Hu et al. (1993) have used solid-state <sup>15</sup>N nuclear magnetic resonance (NMR) spectroscopy to determine the orientations of each of the indole N-H bonds in the gA channel. Hu et al. (1993) and Koeppe et al. (1993) have also presented preliminary <sup>2</sup>H NMR data for [*d*<sub>5</sub>Trp<sup>11</sup>]gA, which are consistent with the <sup>15</sup>N data.

This article will focus on the average orientations of the Trp<sup>9</sup> and Trp<sup>11</sup> rings, using solid-state <sup>2</sup>H NMR spectroscopy, molecular modeling, and the published N-H orientations (Hu et al., 1993). Sets of allowed orientations have been determined for each indole ring. The results are consistent with orientations that, for both rings, are remarkably similar in dimyristoyl phosphatidylcholine (DMPC) and sodium dodecyl sulfate (SDS) environments. During the course of the data analysis, it was also found that the motional properties of these two Trp rings differ significantly, with Trp<sup>9</sup> exhibiting increased flexibility.

## MATERIALS AND METHODS

Ring-*d*<sub>5</sub>-L-Trp was purchased from Cambridge Isotope Laboratories (Cambridge, MA), and was converted to the 9-fluorenylmethoxycarbonyl derivative by the method of Fields et al. (1989). Samples of gA, specifically labeled with ring-*d*<sub>5</sub>-L-Trp at position 9 or position 11, were prepared and purified by standard methods of solid-phase synthesis and liquid chromatography (Becker et al., 1991; Koeppe et al., 1992).

Oriented, hydrated samples of 30  $\mu$ mol of DMPC and 3  $\mu$ mol of labeled gA were prepared between glass plates, as previously described (Killian et al., 1992). <sup>31</sup>P NMR spectra indicated that the lipids in the bilayers became well aligned following 48–72 h of incubation at 40°C. <sup>2</sup>H NMR spectra were recorded at 40°C as previously described (Killian et al., 1992), using the

Received for publication 20 August 1993 and in final form 5 October 1993.

Address reprint requests to Dr. Roger Koeppe, Department of Chemistry and Biochemistry, 103 Chemistry Building, University of Arkansas, Fayetteville, AR 72071.

*Abbreviations used:* gA, gramicidin A; DMPC, dimyristoyl-*sn*-glycero-3-phosphocholine; NMR, nuclear magnetic resonance.

© 1994 by the Biophysical Society

0006-3495/94/01/14/11 \$2.00

quadrupolar echo sequence (Davis et al., 1976) on a Bruker MSL 300 spectrometer with a 7.5-mm-diameter solenoid coil. Between 0.5 million and 1.5 million scans were accumulated while employing a 4- $\mu$ s 90° pulse, a 50–200-ms interpulse time, and a 60- $\mu$ s echo delay time. The signal-to-noise ratio was increased by applying a 1-kHz linebroadening prior to Fourier transformation and by symmetrizing the spectra. The nonsymmetrized spectrum in Fig. 3 was recorded similarly using a Bruker ASX-300 spectrometer.

## Data analysis

Spectra were recorded with the normal to the glass plates either parallel ( $\beta = 0^\circ$ ) or perpendicular ( $\beta = 90^\circ$ ) to the magnetic field,  $H_0$ . Quadrupolar splittings were converted to orientation angles for the C-D bonds using the relation (Killian et al., 1992)

$$\Delta\nu_q = (3/2) (e^2qQ/h) (\frac{1}{2}[3 \cos^2 \theta - 1]) (\frac{1}{2}[3 \cos^2 \beta - 1]), \quad (1)$$

in which  $\theta$  is the angle between a C-D bond and the channel axis, and  $\beta$  is defined above. In this approximation it is assumed that no motional averaging occurs except by fast reorientation of the gramicidin channel about its long axis, and that this motional axis is parallel to the glass plate normal. From this equation it follows that, for the  $\beta = 90^\circ$  sample orientation, splittings are reduced twofold from those observed when  $\beta = 0^\circ$ . The constant ( $e^2qQ/h$ ) is close to 180 kHz for aromatic ring deuterons (Gall et al., 1981). Although the principal component of the spin interaction tensor is along the C-D bond, there is a small off-bond component (Gall et al., 1981). Because the off-bond minor component of the tensor is small in magnitude ( $\eta \approx 0.05$ ) (Gall et al., 1981) and of unknown orientation, we made the approximation of resorting to the use of a symmetric tensor for our analysis.

Based on Eq. 1, the angles  $\theta$  associated with the observed quadrupolar splittings can be calculated, using either a (+) or (-) sign for  $\Delta\nu_q$ . Initially, the proper scheme for assigning these angles to particular ring C-D bonds is unknown. To approach the assignment problem, the coordinates of an energy-minimized Arsen'ev model were used as a starting point (see Killian et al., 1992). A program was written in Fortran77 to rotate a given side chain in orthogonal coordinates about the C $\alpha$ -C $\beta$  bond ( $\chi_1$  torsion angle) and the C $\beta$ -C $\gamma$  bond ( $\chi_2$ ; defined according to the IUPAC-IUB, 1970) in small increments and then, at each orientation, to determine each of the C-D bond orientations and compare with the orientations derived from the quadrupolar splitting data. Typically,  $\chi_1$  and  $\chi_2$  were incremented in 1° intervals; side chain rotation was accomplished using direction cosines (Korn and Korn, 1968).

For each side chain orientation, assignments of bonds to the quadrupolar splitting data were made in two passes: First, the angle of each bond at a particular value of  $\chi_1$  and  $\chi_2$  was compared with the calculated angles associated with the possible (+) and (-) signs of each quadrupolar interaction; then for each interaction the closest angle with each bond was noted, and to all combinations of a particular bond and  $\Delta\nu_q$  value an assignment parameter was given either a (+) or a (-) sign, corresponding to the sign of the interaction. Then, in pass two, it was determined which angle, and which  $\Delta\nu_q$  value it was derived from (with the sign already determined), most closely agreed with the particular bond orientation in the model. The difference between the C-D bond angle in the model and the (best) angle from the  $\Delta\nu_q$  values was then calculated and labeled as the deviation for that particular bond and that particular side chain orientation.

Regions of ( $\chi_1, \chi_2$ ) space where there was good agreement between the model and the experimental data were determined by two criteria: (a) The C2-D, C4-D, C5-D and C6-D bonds of the indole ring should be assigned to different values of  $\Delta\nu_q$ , that is, all of the data points should be used.<sup>1</sup>

Generally, if these assignments were not all different, the particular side chain orientation was discarded from further consideration (unless two of the  $\Delta\nu_q$  values were very close). (b) The sum of the squares of the deviations between the bond orientation angles from the model and from the  $^2\text{H}$  NMR data was calculated for each side chain orientation that was allowed under criterion one, according to the equation

$$\text{"sumsq"} = \sum (\theta_{\text{model}} - \theta_{\text{exp}})^2, \quad (2)$$

where  $\theta_{\text{model}}$  and  $\theta_{\text{exp}}$  are the bond orientation angles with respect to the gA channel's helix axis in the model and from the NMR data, respectively. Favorable orientations have minimal values of "sumsq." To achieve proper weighting when applying Eq. 2, only one of the C4-D and C7-D bonds was included in the calculation;<sup>1</sup> in cases where the NMR signal due to these two deuterons is observed to split (see Fig. 3, and Hu et al., 1993), an average value of  $\Delta\nu_q$  is used.

Information is also available concerning the ring N-H bond orientations (Hu et al., 1993). These data were also included in the least-squares calculation of Eq. 2, by comparing the N-H orientation calculated for the side chain in the model to the published value.

For each of the tryptophans, the allowed orientations were sorted in order of increasing "sumsq" (Eq. 2) and printed in tabular form for inspection. Contour plots showing levels of constant (1/sumsq) as a function of  $\chi_1$  and  $\chi_2$  were prepared using the program Axum (Trimetrix, Inc., Seattle, WA).

The side chain orientations having the lowest values of "sumsq" were displayed attached to the backbone of a minimized Arsen'ev model for gA (Killian et al., 1992) on an Iris-4D computer (Silicon Graphics Corp., Mountain View, CA), using the program InsightII (Biosym Technologies, San Diego, CA).

## RESULTS

### Trp<sup>11</sup>

Fig. 1 shows the  $^2\text{H}$  NMR spectra for an oriented sample of [ $d_5$ -Trp<sup>11</sup>]gA in DMPC, with the membranes oriented at  $\beta = 90^\circ$  or  $\beta = 0^\circ$ . For a  $\beta = 0^\circ$  alignment, with the membrane normal parallel to the magnetic field, distinct quadrupolar splittings are expected for the ring deuterons, each corresponding to a well-defined average orientation of a particular C-D bond with respect to the helix axis. Because the indole ring is planar and the C-D bonds at positions 4 and 7 are colinear (*para* to each other), their resonances will approximately overlap, and only four signals are to be expected (with axially symmetric tensors) from the five C-D bonds of the ring. For the  $\beta = 90^\circ$  orientation, a twofold reduction is expected of all values of  $\Delta\nu_q$ , when the helix axis is aligned parallel to the membrane normal and gA is undergoing fast axial reorientation (Smith and Cornell, 1986; Datema et al., 1986; Nicholson et al., 1987; Killian et al., 1992).

In the  $\beta = 90^\circ$  spectrum (Fig. 1 A), three clear pairs of resonances are evident, corresponding to quadrupolar splittings ( $\Delta\nu_q$ ) of 22, 49, and 95.5 kHz. (The small peak at 0 Hz should probably be attributed to residual HOD in the sample.) When the sample is turned by 90° to give the spectrum at  $\beta = 0^\circ$  (Fig. 1 B), several things happen: (i) there is the expected twofold increase in each of the  $\Delta\nu_q$  values; (ii) the resonance at ( $2 \times 95.5$ ) kHz becomes difficult to observe with our experimental set-up, due to a power roll-off (Griffin, 1981) and/or a small value of  $T_2$ ; (iii) a new resonance appears at 83 kHz.

Taken together, the  $\beta = 0^\circ$  and  $\beta = 90^\circ$  spectra (Fig. 1) indicate four resonances for [ $d_5$ -Trp<sup>11</sup>]gA. The values of  $\Delta\nu_q$

<sup>1</sup> In a planar indole ring, with axially symmetric tensors, the value of  $\Delta\nu_q$  for the C7-D bond would be identical to that for the C4-D bond. Nonaxial tensors (or slightly different values of the quadrupolar coupling constant at different ring positions, or small deviations from planar ring geometry) could, however, make these values slightly different in some spectra; for example, see Fig. 3. The numbers for the ring positions are indicated below Table 2.

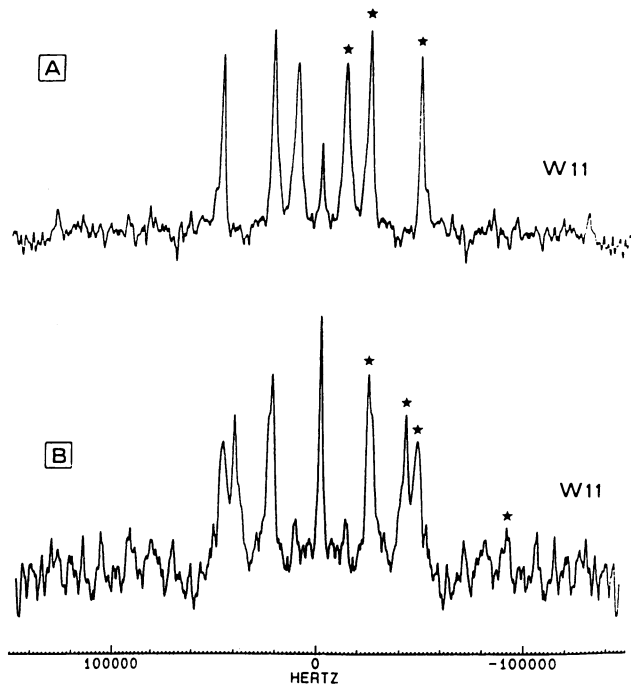


FIGURE 1  $^2\text{H}$  NMR spectra at 46 MHz of an oriented sample of  $[\text{d}_5\text{-Trp}^{11}]\text{gA}$  in DMPC at  $\beta = 90^\circ$  (A) or  $\beta = 0^\circ$  (B); 10:1 lipid:peptide,  $40^\circ\text{C}$ . One member of each pair of resonances in the symmetrized spectra is marked with an asterisk (\*). The peak at 0 Hz is attributed to residual HOD.

associated with these resonances ( $\beta = 0^\circ$  sample orientation) and the corresponding C-D bond orientation angles are summarized in Table 1. From Eq. 1 it follows that the sign of the quadrupolar interaction must be positive for the 191 kHz resonance, whereas for the other resonances the sign may be either positive or negative. A priori, we have no way of assigning the magnitude or the sign of a particular quadrupolar interaction to a particular ring C-D bond. The assignments were made, as described in Materials and Methods, by rotating the  $\text{Trp}^{11}$  side chain through all possible  $\chi_1$  and  $\chi_2$  angles and calculating the agreement between the ring orientation and the  $^2\text{H}$  NMR data at each position, while also including the agreement with the published  $\text{Trp}^{11}$  N-H bond orientation of  $36^\circ$  (Hu et al., 1993) in the least-squares procedure (see Materials and Methods).

Fig. 2 shows the results of the  $(\chi_1, \chi_2)$  search for  $[\text{d}_5\text{Trp}^{11}]\text{gA}$  in the form of a contour plot, contoured in increments of constant  $(1/\text{sumsq})$ , defined in Eq. 2. The results indicate that eight possible ring orientations are consistent

**TABLE 1** Quadrupolar splittings and associated orientation angles for  $[\text{d}_5\text{Trp}^{11}]\text{gA}$

$\Delta\nu_q^*$ kHz	Angle <sup>†</sup> (deg.)
$\pm 44$	48.3 or 61.7
$\pm 83$	42.8 or 69.0
$\pm 98$	40.7 or 72.4
191	26.4

\*  $\beta = 0^\circ$  molecular orientation.

† Angles calculated using a quadrupolar coupling constant of 180 kHz.

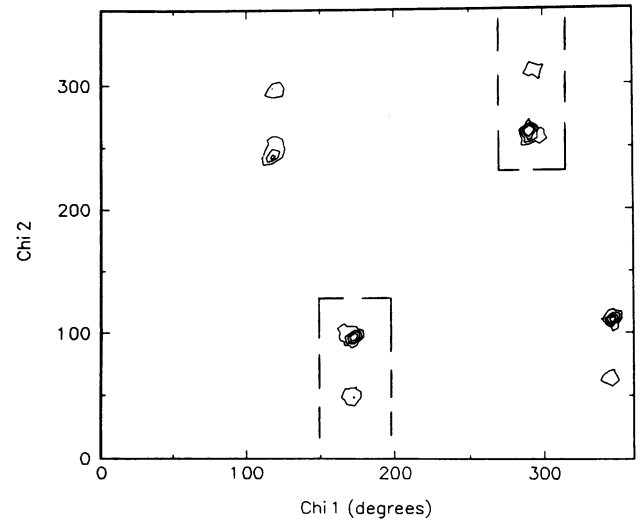


FIGURE 2 Contour plot of the most probable values for the torsion angles  $\chi_1$  and  $\chi_2$  for  $[\text{d}_5\text{Trp}^{11}]\text{gA}$ . The contours are drawn at intervals of 0.015 in units of  $1/\text{sumsq}$ , as defined in equation 1 in the text.  $\text{sumsq}$  is calculated based on both the N-H bond orientation and the C-D bond orientations. Regions of "chi-space" where the N-H is pointing outward toward the surface of the membrane are boxed.

with the NMR data. At four different  $\chi_1$  values, a pair of  $\chi_2$  values is possible. Four of these orientations, those with  $\chi_1$  of  $120^\circ$  or  $344^\circ$ , have the indole N-H group pointing in toward the center of the membrane, in a manner that is inconsistent (see Discussion) with many of the known properties of gramicidin channels, including the conductances of Trp-substituted analogues (Becker et al., 1991), channel formation properties (O'Connell et al., 1990), and Raman spectra (Takeuchi et al., 1990; see Discussion). The other four orientations, those with  $\chi_1$  of  $170^\circ$  or  $296^\circ$  (boxed in Fig. 2), have the indole N-H group pointing out toward the surface of the membrane. We conclude that the  $\text{Trp}^{11}$  ring is oriented according to one of these latter positions. The contour levels in Fig. 2 suggest that the orientations with  $(\chi_1 = 170^\circ, \chi_2 = 93^\circ)$  or  $(\chi_1 = 296^\circ, \chi_2 = 264^\circ)$  are slightly more likely than those with  $(\chi_1 = 170^\circ, \chi_2 = 53^\circ)$  or  $(\chi_1 = 296^\circ, \chi_2 = 309^\circ)$ .

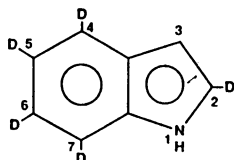
Each of the orientations indicated by the contoured peaks in Fig. 2 involves the same scheme for assigning quadrupolar interactions to the C-D bonds of the  $[\text{d}_5\text{Trp}^{11}]\text{gA}$  ring. The magnitudes and signs of these assignments are given in Table 2. These assignments are in agreement with those of Hu et al. (1993). With these assignments, it is evident that the resonance of the C2 deuteron is observed at  $\beta = 0^\circ$  but not at  $\beta = 90^\circ$ . A similar loss intensity was observed for C5 and C6 of  $\text{Trp}^9$  (see below).

As a direct result of the least-squares procedure, the ring C-4 and C-7 bonds of  $\text{Trp}^{11}$  (labeled in Table 2) were assigned a  $\Delta\nu_q$  value of  $+44$  kHz (for  $\beta = 0^\circ$ ). Additional evidence for this assignment comes from the spectrum shown in Fig. 3, which was recorded on a Bruker ASX-300 spectrometer. With the improved frequency resolution in this spectrum, perhaps due to a better oriented sample, the resonances at  $\pm 22$  kHz are seen to divide into two peaks each.

**TABLE 2** Magnitudes and signs of quadrupolar interactions and corresponding bond orientation angles for the ring C-D bonds\* of Trp<sup>11</sup> and Trp<sup>9</sup>

Ring position	Trp-11		Trp-9	
	$\Delta\nu_q$ (kHz)	Angle <sup>‡</sup> (deg.)	$\Delta\nu_q$ (kHz)	Angle <sup>‡</sup> deg.
C2	83	42.8	-88	73.5
C4, 7	44	48.3	152	28.7
C5	191	26.4	44	47.3
C6	-98	72.4	-104	79.3
N-H <sup>§</sup>		36.0		28.0

\* The ring positions are numbered as shown:



<sup>‡</sup> Orientation angles calculated using Eq. 1, a static quadrupolar coupling constant of 180 kHz for Trp-11, and a motionally reduced constant of 155 kHz for Trp-9 ( $m = 0.86$ ; see text).

<sup>§</sup> N-H orientation angles from the <sup>15</sup>N data of Hu et al. (1993). The Trp-9 angle is reduced to 28° due to the presumed motion.

This assignment, and the splitting of this particular resonance, have also been reported by Hu et al. (1993); our least-squares fit has independently led to the same assignment with no prior assumptions, and Fig. 3 confirms the spectral observation using an independent sample. We attribute the split peak to the asymmetry of the ring C-D interaction tensors, or to slight differences in the magnitude of the quadrupolar coupling constant at the different ring positions. The C7-D bond is closer to the N-H bond than is the C4-D bond (Table 2), and this probably leads to different tensor asymmetries (or magnitudes) and consequently to slightly different magnitudes of  $\Delta\nu_q$  for the C4-D and C7-D bonds. At present, we have no way of deciding how the individual components of the divided resonance should be individually assigned to the C4 and C7 bonds.

We found that it was necessary to consider either the N-H bond orientation (Hu et al., 1993) or the C4, C7 assignment to arrive at the (unique) spectral assignments shown in Table 2. If neither of these is known, then the side chain rotation search gives eight additional possible ring orientations. The “new” peaks in a ( $\chi_1, \chi_2$ ) plot involve different ways of assigning the quadrupolar interactions to the C-D bonds, but each of the “new” peaks also exhibits a discrepancy (in some cases up to 40°) with the known N-H orientation, and with the C4, C7 assignment, and must therefore be excluded from further consideration.

### Effects of small changes in the backbone structure

In the model of Arsen'ev et al. (1986) for the gA channel in SDS micelles, and in the further minimized model that we

used (Killian et al., 1992), the peptide planes show considerable variation in their degrees of tilt with respect to the helix axis. This is reflected in a tabulation of the angles between each of the C $\alpha$ -H bonds and the helix axis (Table II of Killian et al., 1992). As a (small) test of the backbone dependence of the Trp<sup>11</sup> ring orientation, we repeated the least-squares search using the <sup>2</sup>H NMR data for Trp<sup>11</sup> (Table 1) but the backbone for Trp<sup>9</sup> (see Table II of Killian et al., 1992). The results of this calculation agreed with the contour plot of Fig. 2 (data not shown), that is, a 3° change in the tilt of the backbone peptide plane did not change the preferred sets of ( $\chi_1, \chi_2$ ) for the side chain. We cannot exclude the possibility that larger variations in backbone structure could alter the analysis of the side chain orientations with respect to NMR data, but we believe that the differences between the Trp<sup>11</sup> and Trp<sup>9</sup> (see below) orientations noted here are *not* due to backbone differences.

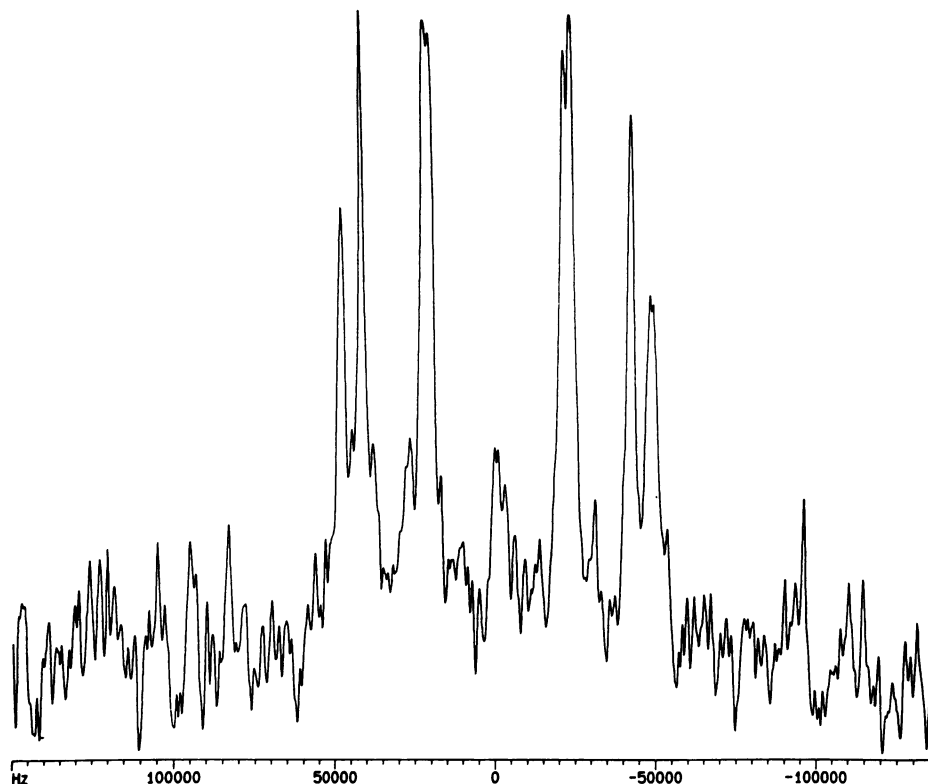
### Trp<sup>9</sup>

Fig. 4 shows the <sup>2</sup>H NMR spectra for an oriented sample of [d<sub>5</sub>-Trp<sup>9</sup>]gA in DMPC. In the  $\beta = 0^\circ$  spectrum (Fig. 4 B), four distinct pairs of resonances are evident, with  $\Delta\nu_q$  values of 44, 88, 104, and 152 kHz. When the sample is turned to  $\beta = 90^\circ$ , one of the central resonances disappears, three peaks are seen, and the resonance at 22 kHz has quite a low intensity.

An attempt was made to assign the magnitudes and signs of the quadrupolar interactions to the C-D bonds of the d<sub>5</sub>-Trp<sup>9</sup> ring, using the least-squares method described above for Trp<sup>11</sup>. When a static quadrupolar coupling constant of 180 kHz was used and when the N-H bond orientation was assumed to be 32°, as determined by Hu et al. (1993), no satisfactory fit could be found. Instead, it was necessary to assume a small extent of motion of the Trp<sup>9</sup> ring that would reduce the observed quadrupolar splittings and reduce the N-H angle. (If there is motion, then the average angle of the N-H bond in this case will be smaller than that determined under the assumption of no motion (Hu et al., 1993)). Table 3 shows the variation in the angles that are calculated from the Trp<sup>9</sup> quadrupolar splittings as small amounts of motional averaging, which would reduce each of the quadrupolar splittings to the same relative extent, are considered. A motion parameter of 0.86 was found to fit both the <sup>2</sup>H and the <sup>15</sup>N NMR data; that is, when both the quadrupolar splittings and the <sup>15</sup>N-H dipolar coupling (Hu et al., 1993) were assumed to be observed at 0.86 of their true values due to motion, a fit was found. For the N-H bond this assumption leads to an angle of 28°.

The allowed sets of ( $\chi_1, \chi_2$ ) angles that we determined for Trp<sup>9</sup> are illustrated in the contour plot of Fig. 5. As with Trp<sup>11</sup>, four allowed ring orientations, those with  $\chi_1$  of 194° or 260° (boxed in Fig. 5), were found to have the indole N-H group pointing out toward the surface of the membrane. Again, four additional ring orientations were found to have the Trp<sup>9</sup> N-H directed toward the center of the membrane, but these were rejected based on other previous data (see

FIGURE 3 A  $^2\text{H}$  NMR spectrum of  $[\text{d}_5\text{-Trp}^{11}]\text{gA}$  to show the split peak near  $\pm 22$  kHz. Sample and conditions as in Fig. 1 B, except that this spectrum was recorded using a Bruker ASX-300 spectrometer.



Discussion). All of the allowed  $\text{Trp}^9$  average ring orientations (Table 2) differ in  $\chi_1$  by  $25^\circ$ - $35^\circ$  from the corresponding orientations for  $\text{Trp}^{11}$  (compare Figs. 2 and 5). Additionally, as noted above, the indole ring of  $\text{Trp}^9$  apparently is subject to more motion than is the ring of  $\text{Trp}^{11}$ .

With the ring C-D bonds of  $\text{Trp}^9$  assigned, it is evident that the resonances of the C5 and C6 deuterons become weak (or nonexistent) in the  $\beta = 90^\circ$  sample orientation. This situation should be compared to the case of  $\text{Trp}^{11}$  (above) in which the C2 resonance disappeared at  $\beta = 90^\circ$ . We do not currently understand these effects. They may be due to an unusual relaxation mechanism.

## DISCUSSION

Several NMR methods are now converging to accurately define the structure of the  $\text{gA}$  channel in aqueous membrane and membrane-like environments. The first method is the two-dimensional  $^1\text{H}$  NMR analysis of the channel structure in SDS micelles (Arsen'ev et al., 1985, 1986; Lomize et al., 1992). This method has served to accurately define the right-handed  $\beta^{6.3}$ -helical fold of the  $\text{gA}$  backbone in the SDS environment. The similar circular dichroism spectra for  $\text{gA}$  in SDS and phospholipid environments was a direct indication that the backbone folding pattern and helix sense are similar in the two environments (Arsen'ev et al., 1985). This was later confirmed by solid-state NMR spectroscopy (see below). Of less certainty are the  $\text{gA}$  side chain orientations and whether the orientations and/or motions of side chains should be the same in detergents and membranes.

Solid-state NMR provides a second approach to the  $\text{gA}$  structure, an approach that can be applied in phospholipid membranes.  $^{13}\text{C}$ - (e.g., Smith and Cornell, 1986; Separovic et al., 1991),  $^{15}\text{N}$ - (e.g., Nicholson and Cross, 1989; Nicholson et al., 1991), and  $^2\text{H}$ -labeled (MacDonald and Seelig, 1988; Hing et al., 1990a,b; Prosser et al., 1991; Killian et al., 1992; Hu et al., 1993) samples of  $\text{gA}$  have been investigated. In DMPC bilayers,  $\text{gA}$  exhibits the  $\beta^{6.3}$  channel conformation and rotates rapidly about the helix axis (Smith and Cornell, 1986; Datema et al., 1986; Nicholson et al., 1987; MacDonald and Seelig, 1988), at a rate of  $\sim 1.5 \times 10^8 \text{ s}^{-1}$  (Prosser, 1992). The ability of the hydrated, membrane-incorporated  $\text{gA}$  to orient between glass plates (Nicholson et al., 1987) allows accurate geometrical information about the labeled bonds to be derived from NMR measurements in which the angle between the magnetic field and the axis of molecular reorientation is known. This applies for labeled bonds in the backbone as well as in the side chains. The purpose of such measurements has been severalfold: (i) to determine backbone peptide plane orientations in DMPC (Nicholson and Cross, 1989; Chiu et al., 1991; Ketchem et al., 1993) and compare them with those determined in SDS; (ii) to examine overall molecular motion (Smith and Cornell, 1986; MacDonald and Seelig, 1988; Lee et al., 1993); (iii) to examine the orientations of individual side chains (Killian et al., 1992; Hu et al., 1993); and (iv) to assess the local motions of backbone and side chain groups.

This study has focused on the indole rings of  $\text{Trp}^9$  and  $\text{Trp}^{11}$  of the  $\text{gA}$  channel in DMPC bilayers, using  $^2\text{H}$  NMR. Our main findings are: (a) The  $^2\text{H}$  quadrupolar splittings

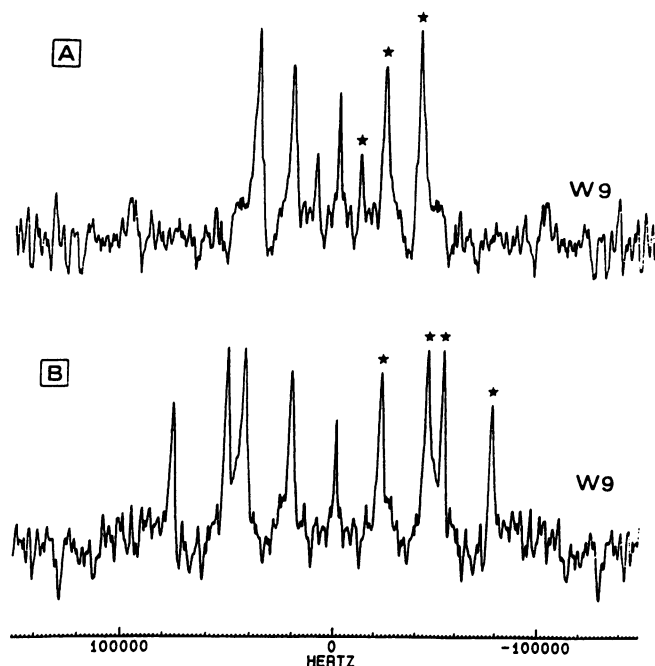


FIGURE 4  $^2\text{H}$  NMR spectra at 46 MHz of an oriented sample of  $[\text{d}_5\text{-Trp}^9]\text{gA}$  in DMPC at  $\beta = 90^\circ$  (A) or  $\beta = 0^\circ$  (B). 10:1 lipid:peptide,  $40^\circ\text{C}$ . One member of each pair of resonances in the symmetrized spectra is marked with a \*. The peak at 0 Hz is attributed to residual HOD.

alone were not sufficient to make unique spectral assignments and define the indole ring orientations; we also had to consider either the N-H bond orientations or the C4/C7 deuteron assignment. (b) The ring of  $\text{Trp}^{11}$  is essentially immobile, whereas the ring of  $\text{Trp}^9$  exhibits significant motion. (c) The orientations of the  $\text{Trp}^9$  and  $\text{Trp}^{11}$  rings are now very well defined. The ring orientations also correlate with unique assignments for the magnitudes and signs of each of the ring C-D bond quadrupolar interactions. Each of these ring orientations can be achieved using eight different sets of  $(\chi_1, \chi_2)$ , four of which are consistent with other spectroscopic and functional studies, and one of which is in agreement with the two-dimensional  $^1\text{H}$  NMR data for gA in SDS (Arsen'ev et

TABLE 3 Variation of  $[\text{d}_5\text{Trp}^9]\text{gA}$  orientation angles as a function of motional averaging

$\Delta\nu_q^*$ (kHz)	Angle (degrees)		
	$m = 1.00^\ddagger$	$m = 0.92$	$m = 0.86$
44	48.3	47.8	47.3
-44	61.7	62.4	62.9
88	42.1	41.0	40.0
-88	70.1	71.8	73.5
104	39.8	38.5	37.3
-104	73.9	76.5	79.3
152	32.7	30.6	28.7
N-H	32.0 $^\S$	30.0	28.0

\*  $\beta = 0^\circ$  molecular orientation.

$^\ddagger$  The effective quadrupolar coupling constant is  $(m \times 180)$  kHz.

$^\S$  An angle of  $32^\circ$  for the  $\text{Trp}^9$  indole N-H is taken from Hu et al. (1993), who assumed no motion.

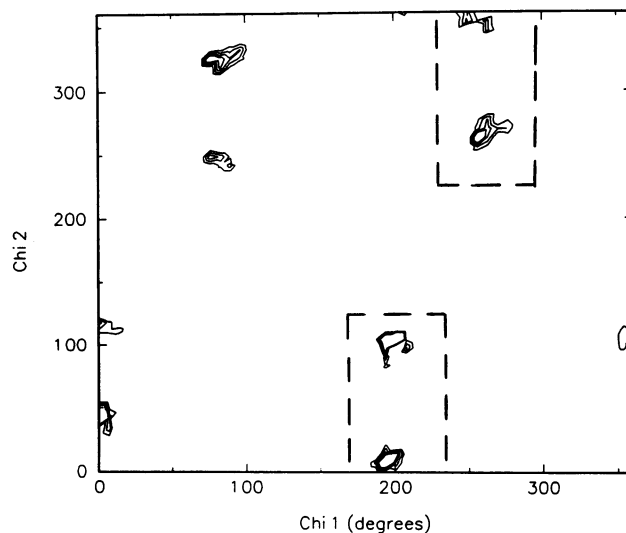


FIGURE 5 Contour plot of the most probable values for the torsion angles  $\chi_1$  and  $\chi_2$  for  $[\text{d}_5\text{Trp}^9]\text{gA}$ . The contours and boxes are drawn as described in Fig. 2.

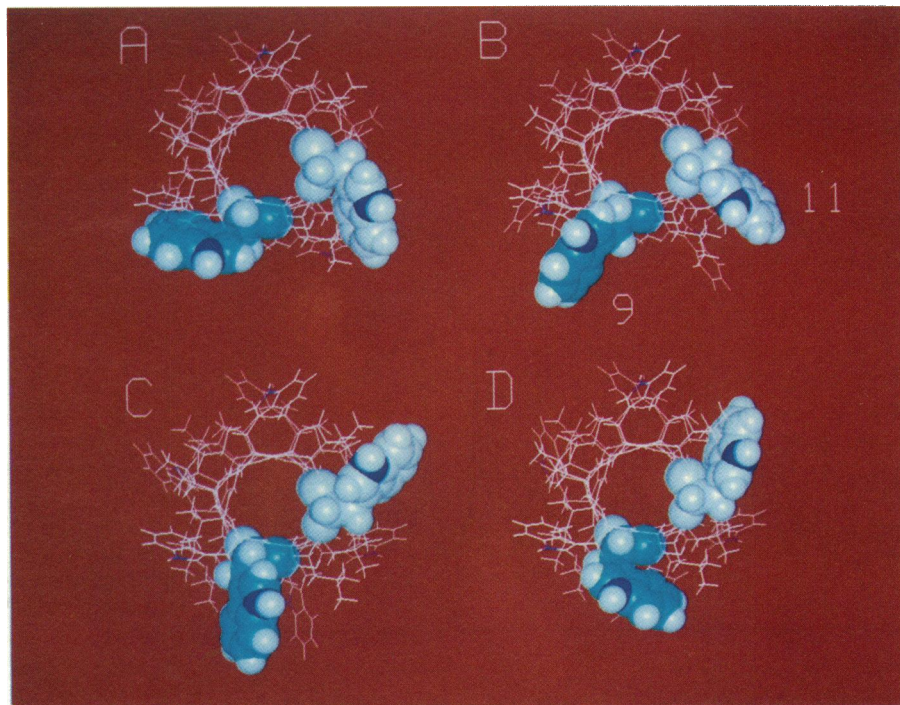
al., 1986; Lomize et al., 1992) but is more precisely defined. Together, the  $^1\text{H}$ ,  $^2\text{H}$ , and  $^{15}\text{N}$  NMR data suggest that the  $\text{Trp}^9$  and  $\text{Trp}^{11}$  ring orientations may be quite similar in the SDS and DMPC environments. (d) The experimental C-D bond orientation angles, derived assuming an axially symmetric quadrupolar interaction tensor, show small but systematic deviations from the angles that are calculated from a "best-fit" model. Each of these findings will be discussed in turn.

### Requirements to assign the C-D quadrupolar interactions and uniquely define the indole ring orientations

We used two types of information to uniquely assign the  $^2\text{H}$  quadrupolar interactions for the tryptophans: the magnitudes of the quadrupolar splittings from  $^2\text{H}$  NMR spectra and the orientation of the ring N-H bond derived from  $^{15}\text{N}$  NMR data (Hu et al., 1993). To make unique assignments, we need either the approximate N-H orientation or the C4/C7  $^2\text{H}$  assignment. For  $\text{Trp}^{11}$  both pieces of starting information are available, they are self-consistent in that they lead to the same assignments, and only one of them is needed. For  $\text{Trp}^9$ , the available spectra give no clue as to the C4/C7 assignment, and we must assume an approximate orientation for the N-H.

For ring-labeled  $\text{d}_5\text{-L-Trp}$ , four pairs of resonances are expected (or possibly five pairs, if the signals from the C4 and C7 deuterons are distinguishable; see Fig. 3). Initially, one has no simple way to match the resonances with the ring C-D bonds, unless the closely spaced resonances due to the C4 and C7 deuterons are distinguishable. Even if C4 and C7 can be easily assigned (Hu et al., 1993), a systematic procedure may be required to assign the other three resonances. For  $\text{Trp}^{11}$ , although we made no a priori assumption about the C4 and C7 assignments, our least-squares procedure nev-

**FIGURE 6** Models that show CPK representations of the four most probable orientations for Trp<sup>9</sup> and Trp<sup>11</sup> of gA, on a wire framework of the rest of the molecule. The orientations correspond to the peaks in the boxed regions of the contour plots of Figs. 2 and 5. The backbone model is the minimized Arsen'ev model previously described (Killian et al., 1992); the other side chains are in the orientations of Arsen'ev et al. (1986). The values of ( $\chi_1$ ,  $\chi_2$ ) associated with each orientation are, for Trp<sup>9</sup>: (A) (260°, 269°); (B) (260°, 348°); (C) (194°, 13°); (D) (194°, 92°); and for Trp<sup>11</sup>: (A) (295°, 264°); (B) (295°, 309°); (C) (170°, 50°); (D) (170°, 95°). The orientations for Trp<sup>9</sup> and Trp<sup>11</sup> are uncorrelated; that is, the <sup>2</sup>H NMR data are consistent with any of the four Trp<sup>9</sup> orientations being associated with any of the four Trp<sup>11</sup> orientations. The model of Arsen'ev et al. (1986) has Trp<sup>11</sup> near orientation B and Trp<sup>9</sup> near orientation D in the figure. The model was displayed using the program InsightII (Biosym.) on an Iris-4D computer (Silicon Graphics).



ertheless arrived at a unique set of assignments that correlated the C4 and C7 deuterons with the  $\pm 22$  kHz peaks that divide in Fig. 3. For Trp<sup>9</sup>, the <sup>2</sup>H NMR spectra gave no hint as to the C4 and C7 assignments (because their resonances appeared to overlap perfectly; Fig. 4), but our procedure was still able to give unique assignments for the Trp<sup>9</sup> ring (Table 2). The procedure should be generally applicable to the other tryptophans of gA and to other labeled tryptophans in proteins where the backbone geometry can be oriented and defined (e.g., transmembrane helices or sheets).

### Trp<sup>9</sup> is more mobile than Trp<sup>11</sup>

The Trp<sup>11</sup> ring could be assigned without assuming any motional averaging of the quadrupolar interaction. This is remarkable since some averaging should be expected to occur, based on the measured order parameter of gA in DMPC bilayers of  $\sim 0.93$  (see Separovic et al., 1993, and references therein). It has been suggested that “wobbling” motions of gA about the helix axis are responsible for the small extent of motional averaging that has been observed for various labeled sites (Hing et al., 1990a,b; Prosser et al., 1991; Killian et al., 1992) in the peptide backbone (Prosser, 1992). Such motions of the entire molecule should also lead to motional averaging of labeled sites in the side chains. For Trp<sup>9</sup> indeed such motional averaging had to be assumed in order to obtain a fit of both the <sup>2</sup>H NMR and the <sup>15</sup>N NMR data.

Our results therefore suggest that Trp<sup>11</sup> is more rigid than the gA molecule as a whole in a bilayer of DMPC. The physical basis for this observation has yet to be determined. One possible explanation is that the Trp<sup>11</sup> side chain is held in a unique position by a network of hydrogen bonds to the lipid head groups and/or carbonyl esters. To allow off-axis

motions of the entire molecule—while at the same time maintaining a fixed orientation for the Trp<sup>11</sup> indole—the  $\chi_1$  and/or  $\chi_2$  torsion angles for residue 11 would have to undergo rapid small adjustments. This may be possible because such adjustments would involve only a few degrees of freedom.

As the entire gA channel rotates, all of the indole rings would need to exchange H-bonding partners, as they make and break hydrogen bonds to different water or lipid molecules. In this process of “H-bond exchange” the ring of Trp<sup>9</sup> is probably less involved because it is buried more deeply within the membrane.

We also note that Trp<sup>11</sup> decreases the average duration (open time) of the ion-conducting gA channel, compared to Phe<sup>11</sup> (Bamberg et al., 1976; Sawyer et al., 1990; Becker et al., 1991), which is unable to hydrogen bond. As suggested by Becker et al. (1991), Trp<sup>11</sup> could destabilize a gA channel by “pulling” a dimer apart, due to hydrogen bonding interactions of the Trp<sup>11</sup> indole ring with the diphytanoylphosphatidylcholine lipid interface. Replacement of Trp<sup>9</sup> by Phe<sup>9</sup> has little effect on the single-channel lifetime (Becker et al., 1991). This result is consistent with our analysis of the NMR data, which indicates that Trp<sup>9</sup> is more mobile than Trp<sup>11</sup>—even in a shorter lipid (DMPC) than that used for the single-channel studies—and therefore that Trp<sup>9</sup> probably is less involved in hydrogen bonding with either of the lipids.

### Torsion angles ( $\chi_1$ , $\chi_2$ ) for the Trp<sup>9</sup> and Trp<sup>11</sup> rings

With the magnitudes and signs of the quadrupolar interactions (and the N-H bond orientations) assigned (Table 2), the ring orientations are defined. Each of these ring angles is

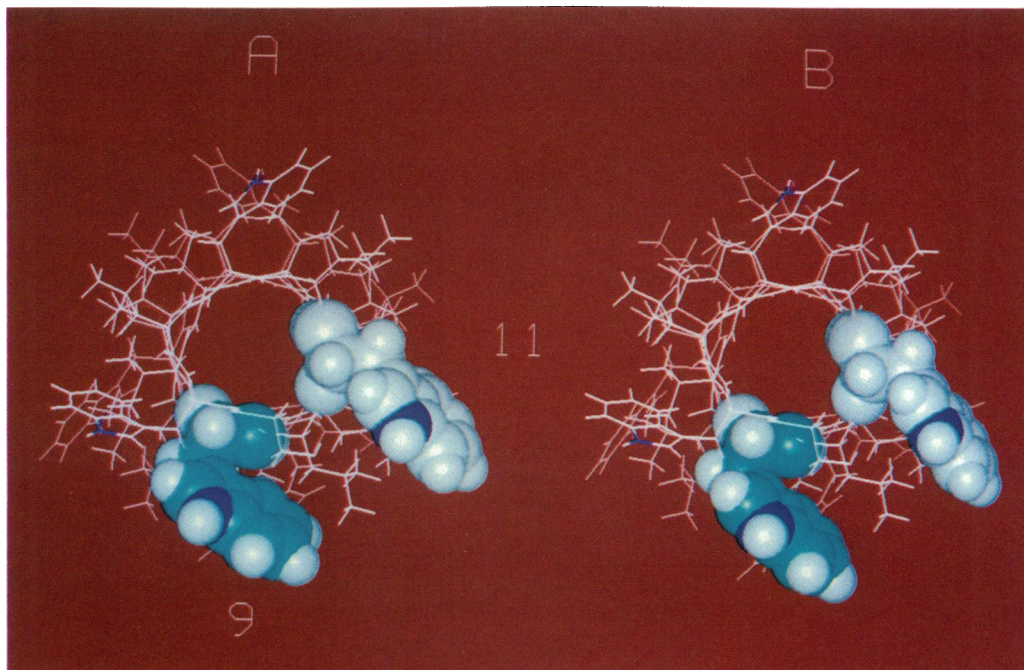


FIGURE 7 Comparison of Trp<sup>9</sup> and Trp<sup>11</sup> orientations from solid-state NMR analysis of oriented gA channels in DMPC (A) with the orientations from two-dimensional NMR analysis of gA dissolved in aqueous SDS (Arsen'ev et al., 1986) (B).

consistent with eight different sets of ( $\chi_1$ ,  $\chi_2$ ) angles for each of the corresponding Trp rings (Figs. 2 and 5).

Those sets of ( $\chi_1$ ,  $\chi_2$ ) angles that have the indole N-H bond (of either Trp<sup>9</sup> or Trp<sup>11</sup>) directed toward the center of the membrane can be excluded for several reasons: (i) A series of single and multiple Trp  $\rightarrow$  Phe substitutions in gA has shown that each of the indole dipoles is oriented so as to interact favorably with incoming cations (Becker et al., 1991, 1992); (ii) gA monomers are slow to diffuse across lipid bilayers (O'Connell et al., 1990) because the Trp's serve to "anchor" the monomers on the side to which they are added, presumably by hydrogen bonding between the indole NH and the lipid head groups at the interface, since various Trp  $\rightarrow$  Phe substituted gramicidins are more freely diffusible (M. D. Becker, O. S. Andersen, and R. E. Koepe, unpublished results); (iii) there is an energetic cost to burying a Trp N-H group too deeply in a membrane, as shown by the short mean lifetime of channels formed by [Trp<sup>1</sup>]gA (Mazet et al., 1984), and by the bias against the formation of double-helical channels by natural gA (Durkin et al., 1992), both of which suggest that the indole N-H does not like to be buried; (iv) using N-<sup>2</sup>H exchange and Raman spectroscopy, Takeuchi et al. (1990) have shown that three of the indole N-H's are accessible to water. (The fourth Trp, presumably Trp<sup>9</sup>, is inaccessible, probably because it is underneath the lipid head groups and shielded from the H<sub>2</sub>O.) After excluding values of ( $\chi_1$ ,  $\chi_2$ ) for which the indole N-H's point inward, we are left with four allowed sets of ( $\chi_1$ ,  $\chi_2$ ) each for Trp<sup>9</sup> and Trp<sup>11</sup> (boxed regions in Figs. 2 and 5).

Fig. 6 shows a wire model of the gA channel dimer with Corey-Pauling-Koltun representations of Trp<sup>9</sup> and of Trp<sup>11</sup> in four different orientations corresponding to the "best-fit"

values of  $\chi_1$  and  $\chi_2$ . The orientations of Trp<sup>9</sup> and Trp<sup>11</sup> in Fig. 6 are uncorrelated with each other; that is, Trp<sup>9</sup> could assume any of the possible orientations regardless of which one is chosen for Trp<sup>11</sup>. (Sixteen panels would be required to show all possible pairwise combinations.) The model of Arsen'ev et al. for gA in SDS (Arsen'ev et al., 1986; Lomize et al., 1992) has Trp<sup>11</sup> near the orientation shown in Fig. 6 B and Trp<sup>9</sup> near the orientation shown in Fig. 6 D. In Fig. 6, A and B,  $\chi_1$  of Trp<sup>11</sup> is constant at 295°, while  $\chi_1$  of Trp<sup>9</sup> is constant at 260°, and two different  $\chi_2$  values are shown for each. Similarly, in Fig. 6, C and D,  $\chi_1$  of Trp<sup>11</sup> is constant at 170°, while  $\chi_1$  of Trp<sup>9</sup> is constant at 194°, and two different  $\chi_2$  values are shown for each.

The present results suggest agreement between the average side-chain orientations of Trp<sup>9</sup> and Trp<sup>11</sup> in DMPC and SDS environments. Orientation B for Trp<sup>11</sup> and orientation D for Trp<sup>9</sup> in DMPC (Fig. 6) agree with the results from the two-dimensional <sup>1</sup>H measurements of gA in SDS (Arsen'ev et al., 1986; Lomize et al., 1992). These orientations are compared in Fig. 7, where the similarity in ring orientations derived by the two methods is striking.

### Asymmetry of the aromatic C-D bond quadrupolar interaction tensor

For each of the four possible orientations for Trp<sup>9</sup> and Trp<sup>11</sup> (Figs. 2, 5, and 6), we calculated the deviation of each C-D or N-H bond orientation in the model (Fig. 6, A–D) from the NMR-based prediction (Table 2). These deviations are listed in Table 4, where it is apparent that the deviations are systematic rather than random. For each of the possible sets of ( $\chi_1$ ,  $\chi_2$ ) values of Trp<sup>11</sup>, the pattern by which the ring bonds



**TABLE 4** Deviations of model C-D bond orientation angles from the predictions of  $^2\text{H}$  NMR for Trp<sup>11</sup> and Trp<sup>9</sup> indole rings at the "best-fit" values of  $\chi_1$  and  $\chi_2^*$ 

$\chi_1$	$\chi_2$	C2-D	C4-D	C5-D	C6-D	N-H
Trp-11 angular deviation (degrees)						
120	253	2.55	2.36	-4.14	0.64	-1.09
120	294	2.52	2.34	-4.16	0.64	-1.09
170	53	2.36	2.14	-4.67	0.61	-1.43
170	93	2.50	2.18	-4.36	0.70	-1.31
296	264	2.39	3.77	-2.98	-0.04	0.64
296	309	2.46	3.78	-2.81	0.02	0.72
344	65	2.63	2.99	-3.37	0.44	-0.24
344	108	2.47	2.94	-3.64	0.37	-0.35
Trp-9 angular deviation (degrees)						
6	36	0.44	1.85	0.66	-0.37	-2.70
6	114	0.49	1.97	0.72	-0.36	-2.63
90	244	0.14	3.21	0.80	0.24	-1.37
90	324	-0.06	3.18	0.52	0.43	-1.64
194	12	0.32	3.00	0.93	0.03	-2.77
194	92	0.11	2.96	0.64	0.22	-1.77
260	268	0.84	2.54	1.35	-0.53	-1.65
260	348	0.44	2.39	0.82	-0.21	-2.19

\* The sets of ( $\chi_1$ ,  $\chi_2$ ) torsion angles correspond to the "NH-out" maxima of Figs. 2 and 5. The reference NMR-predicted angles are given in Table 2. The sign of the deviation indicates whether the angle in the model is larger or smaller than the reference.

differ from the NMR predictions is similar; the same statement can be made for Trp<sup>9</sup>. These patterns suggest a systematic "discrepancy" in the data set or the model.

There are several possible explanations for this phenomenon. First, the NMR predictions assume axially symmetric quadrupolar interaction tensors. This is only an approximation (Gall et al., 1981), since the tensor for aromatic C-D bonds has an asymmetry component of  $\sim 0.05$ . Second, the model assumes planar indole rings. A small deviation is possible. Third, the model assumes a static quadrupolar coupling constant of 180 kHz for all CD bonds. Also here, small deviations are possible. Fourth, small amplitude local motions of the Trp rings could influence the values of  $\Delta\nu_q$  for each of the CD bonds to slightly different extents, depending on the nature of the motion. The deviations listed in Table 4 could result from any or all of the above.

As a group, the Trp<sup>11</sup> bond deviations from the NMR predictions listed in Table 4 are larger than the Trp<sup>9</sup> deviations. This is because several different motion parameters were tried for Trp<sup>9</sup> (Table 3), and the values in Table 4 reflect an optimized situation for  $m = 0.86$ , whereas  $m$  was not varied from 1.00 for Trp<sup>11</sup>. Decreasing  $m$  slightly below 1.00 would improve the "fit" of some of the C-D bonds of Trp<sup>11</sup> in Table 4 (although not the fit of the N-H bond). This does not alter the important conclusion that Trp<sup>9</sup> undergoes substantially more motional averaging than does Trp<sup>11</sup>.

The ring orientations illustrated in Fig. 6 define angles  $\xi$  between the planes of the Trp rings and the helix axis. For Trp<sup>11</sup>,  $\xi$  is 19° (any of the panels in Fig. 6), and for Trp<sup>9</sup>  $\xi$  is 26°. These values are in good agreement with those of Hu et al. (1993), based on  $^{15}\text{N}$  data. Overall, the Trp ring orientations are very well defined by solid-state NMR using oriented samples; the method therefore can also be applied to other protein systems that can be oriented.

## Comparison of NMR methods

If one compares the approaches to Trp side-chain geometry by the methods of two-dimensional  $^1\text{H}$  NMR and solid-state  $^2\text{H}$  NMR, several statements can be made: Both methods yield families of Trp orientations that satisfy the data. For the case of two-dimensional NMR, the family members for a given Trp appear in the same general region of ( $\chi_1$ ,  $\chi_2$ ) space (e.g., Fig. 3 of Lomize et al., 1992). We also have relied on the two-dimensional NMR for the backbone structure (although others have used solid-state NMR approaches to define the backbone structure; cf. Cornell et al., 1988a,b; Nicholson and Cross, 1989; Chiu et al., 1991; Ketchem et al., 1993). The geometrical uncertainties in two-dimensional NMR arise from the uncertainties in the nuclear Overhauser enhancement interactions and from the possibility of molecular motion. For the case of solid-state NMR, the family members for a given Trp conformation appear in four different regions of ( $\chi_1$ ,  $\chi_2$ ) space (boxed regions of Figs. 2 and 5), but each member is rather precisely defined. Again, there is uncertainty due to molecular motion, but the solid-state approach provides a way of estimating the extent of motion (cf. Trp<sup>9</sup> results, above). One can now say, for example, that Trp<sup>9</sup> exhibits more motional averaging than does Trp<sup>11</sup>.

Together the two NMR methods provide a convergent and accurate picture of the side chain geometries and mobilities for the gA channel (Fig. 7). The convergent results also suggest that the gA channel structures in SDS and DMPC environments are highly similar. The solid-state approach, due to its high sensitivity, will also prove valuable as a difference method for examining the effects of sequence changes (e.g., Durkin et al., 1990), fatty acylation (Williams et al., 1992; Vogt et al., 1992; Koeppe et al., 1993), or other covalent modifications to the gramicidin channel. Side chain-side

chain and side chain–lipid interactions are expected to be revealed through changes in the  $^2\text{H}$  NMR spectra that reflect different side chain orientations and/or dynamics. The solid-state approach can in principle also be used to examine the gA channel in different oriented lipid systems.

We thank Olaf S. Andersen for reading the manuscript and Ben de Kruijff, Bas Vogt, and Olaf Andersen for helpful discussions.

This work was supported in part by NIH grant GM34968 from the U.S. Public Health Service and NSF grant RII-8922108. R. E. K. was supported by a Fulbright grant from the Netherlands America Commission for Educational Exchange.

## REFERENCES

- Andersen, O. S., and R. E. Koeppel, II. 1992. Molecular determinants of channel function. *Physiol. Rev.* 72:S89–S158.
- Arsen'ev, A. S., I. L. Barsukov, V. F. Bystrov, A. L. Lomize, and Y. A. Ovchinnikov. 1985. Proton NMR study of gramicidin A transmembrane ion channel. Head-to-head right-handed, single-stranded helices. *FEBS Lett.* 186:168–174.
- Arsen'ev, A. S., A. L. Lomize, I. L. Barsukov, and V. F. Bystrov. 1986. Gramicidin A transmembrane ion-channel. Three-dimensional structure reconstruction based on NMR spectroscopy and energy refinement. *Biol. Membr.* 3:1077–1104.
- Bamberg, E., K. Noda, E. Gross, and P. Läuger. 1976. Single-channel parameters of gramicidin A, B, and C. *Biochim. Biophys. Acta* 419:223–228.
- Becker, M. D., D. V. Greathouse, R. E. Koeppel, II, and O. S. Andersen. 1991. Amino acid sequence modulation of gramicidin channel function: effects of tryptophan-to-phenylalanine substitutions on the single-channel conductance and duration. *Biochemistry*. 30:8830–8839.
- Becker, M. D., R. E. Koeppel, II, and O. S. Andersen. 1992. Amino acid substitutions and ion channel function. Model-dependent conclusions. *Biophys. J.* 62:25–27.
- Chiu, S. W., L. K. Nicholson, M. T. Brennehan, S. Subramaniam, Q. Teng, J. A. McCammon, T. A. Cross, and E. Jakobsson. 1991. Molecular dynamics computations and solid state nuclear magnetic resonance of the gramicidin cation channel. *Biophys. J.* 60:974–978.
- Cornell, B. A., F. Separovic, A. J. Baldassi, and R. Smith. 1988a. Conformation and orientation of gramicidin A in oriented phospholipid bilayers measured by solid state carbon-13 NMR. *Biophys. J.* 53:67–76.
- Cornell, B. A., F. Separovic, and R. Smith. 1988b. Side chain and backbone conformation of gramicidin A in lipid bilayer membranes. In *Transport through Membranes: Carriers, Channels and Pumps*. A. Pullman, J. Jortner, and B. Pullman, editors. Kluwer Academic Publishers, Dordrecht, the Netherlands. 289–295.
- Datema, K. P., K. P. Pauls, and M. Bloom. 1986. Deuterium nuclear magnetic resonance investigation of the exchangeable sites on gramicidin A and gramicidin S in multilamellar vesicles of dipalmitoylphosphatidylcholine. *Biochemistry*. 25:3796–3803.
- Davis, J. H., K. R. Jeffrey, M. Bloom, M. I. Valio, and T. P. Higgs. 1976. Quadrupolar echo deuterium magnetic resonance spectroscopy in ordered hydrocarbon chains. *Chem. Phys. Lett.* 42:390–394.
- Durkin, J. T., R. E. Koeppel, II, and O. S. Andersen. 1990. Energetics of gramicidin hybrid channel formation as a test for structural equivalence: side-chain substitutions in the native sequence. *J. Mol. Biol.* 211: 221–234.
- Durkin, J. T., L. L. Providence, R. E. Koeppel, II, and O. S. Andersen. 1992. Formation of non- $\beta^6\text{-}^3$ -helical gramicidin channels between sequence-substituted gramicidin analogues. *Biophys. J.* 62:145–159.
- Fields, C. G., G. B. Fields, R. L. Noble, and T. A. Cross. 1989. Solid-phase peptide synthesis of  $^{15}\text{N}$ -gramicidins A, B, and C and high performance liquid chromatographic purification. *Int. J. Pept. Protein Res.* 33: 298–303.
- Gall, C. M., J. A. DiVerdi, and S. J. Opella. 1981. Phenylalanine ring dynamics by solid-state  $^2\text{H}$  NMR. *J. Am. Chem. Soc.* 103:5039–5043.
- Griffin, R. G. 1981. Solid state nuclear magnetic resonance of lipid bilayers. *Methods Enzymol.* 72:108–174.
- Hing, A. W., S. P. Adams, D. F. Silbert, and R. E. Norberg. 1990a. Deuterium NMR of Val1...(2- $^2\text{H}$ )Ala3...gramicidin A in oriented DMPC bilayers. *Biochemistry*. 29:4144–4156.
- Hing, A. W., S. P. Adams, D. F. Silbert, and R. E. Norberg. 1990b. Deuterium NMR of 2HCO-Val1...gramicidin A and 2HCO-Val1-D-Leu2... gramicidin A in oriented DMPC bilayers. *Biochemistry*. 29:4156–4166.
- Hu, W., K. C. Lee, and T. A. Cross. 1993. Tryptophans in membrane proteins: indole ring orientations and functional implications in the gramicidin channel. *Biochemistry*. 32:7035–7047.
- IUPAC-IUB Commission on Biochemical Nomenclature. 1970. Abbreviations and symbols for the description of the conformation of polypeptide chains. *J. Mol. Biol.* 52:1–17.
- Ketchum, R. R., W. Hu, and T. A. Cross. 1993. High-resolution conformation of gramicidin A in a lipid bilayer by solid-state NMR. *Science (Washington DC)*. 261:1457–1460.
- Killian, J. A. 1992. Gramicidin and gramicidin/lipid interactions. *Biochim. Biophys. Acta.* 1113:391–425.
- Killian, J. A., M. J. Taylor, and R. E. Koeppel, II. 1992. Orientation of the valine-1 side chain of the gramicidin transmembrane channel and implications for channel functioning. A  $^2\text{H}$  NMR study. *Biochemistry*. 31: 11283–11290.
- Koeppel, R. E., II, L. L. Providence, D. V. Greathouse, F. Heitz, Y. Trudelle, N. Purdie, and O. S. Andersen. 1992. On the helix sense of gramicidin A single channels. *Proteins*. 12:49–62.
- Koeppel, R. E., II, J. A. Killian, T. C. B. Vogt, and D. V. Greathouse. 1993. Tryptophan-lipid interactions in acyl gramicidins analyzed using  $^2\text{H}$  NMR. In 11th International Biophysics Congress, Budapest, Hungary. 132. (Abstr.) Hungarian Academy of Sciences, Budapest.
- Korn, G. A., and T. M. Korn. 1968. *Mathematical Handbook for Scientists and Engineers*. 2nd edition. McGraw-Hill, New York. 473.
- Lee, K.-C., W. Hu, and T. A. Cross. 1993.  $^2\text{H}$  NMR determination of the global correlation time of the gramicidin channel in a lipid bilayer. *Biophys. J.* 65:1162–1167.
- Lomize, A. L., V. Y. Orekhov, and A. S. Arsen'ev. 1992. Refinement of the spatial structure of the ionic channel of gramicidin A. *Bioorg. Khimiya*. 18:182–200. (In Russian)
- MacDonald, P. M., and J. Seelig. 1988. Dynamic properties of gramicidin A in phospholipid membranes. *Biochemistry*. 27:2357–2364.
- Mazet, J. L., O. S. Andersen, and R. E. Koeppel, II. 1984. Single-channel studies on linear gramicidins with altered amino acid sequences. A comparison of phenylalanine, tryptophan, and tyrosine substitutions at positions 1 and 11. *Biophys. J.* 45:263–276.
- Nicholson, L. K., and T. A. Cross. 1989. Gramicidin cation channel: an experimental determination of the right-handed helix sense and verification of  $\beta$ -type hydrogen bonding. *Biochemistry*. 28:9379–9385.
- Nicholson, L. K., F. Moll, T. E. Mixon, P. V. LoGrasso, J. C. Lay, and T. A. Cross. 1987. Solid-state nitrogen-15 NMR of oriented lipid bilayer bound gramicidin A'. *Biochemistry*. 26:6621–6626.
- Nicholson, L. K., Q. Teng, and T. A. Cross. 1991. Solid-state nuclear magnetic resonance derived model for dynamics in the polypeptide backbone of the gramicidin A channel. *J. Mol. Biol.* 218:621–637.
- O'Connell, A. M., R. E. Koeppel, II, and O. S. Andersen. 1990. Kinetics of gramicidin channel formation in lipid bilayers: transmembrane monomer association. *Science (Washington DC)*. 250:1256–1259.
- Prosser, R. S. 1992. Ph.D. thesis, University of Guelph, Guelph, Ontario, Canada.
- Prosser, R. S., J. H. Davis, F. W. Dahlquist, and M. A. Lindorfer. 1991. Deuterium nuclear magnetic resonance of the gramicidin A backbone in a phospholipid bilayer. *Biochemistry*. 30:4687–4696.
- Sarges, R., and B. Witkop. 1965. Gramicidin A. V. The structure of valine- and isoleucine-gramicidin A. *J. Am. Chem. Soc.* 87:2011–2020.
- Sawyer, D. B., L. P. Williams, W. L. Whaley, R. E. Koeppel, II, and O. S. Andersen. 1990. Gramicidins A, B, and C form structurally equivalent ion channels. *Biophys. J.* 58:1207–1212.
- Separovic, F., K. Hayamizu, R. Smith, and B. A. Cornell. 1991. Carbon-13 chemical shift tensor of L-tryptophan and its application to polypeptide structure determination. *Chem. Phys. Lett.* 181:157–162.

- Separovic, F., R. Pax, and B. Cornell. 1993. NMR order parameter analysis of a peptide plane aligned in a lyotropic liquid crystal. *Mol. Phys.* 78: 357-369.
- Smith, R., and B. A. Cornell. 1986. Dynamics of the intrinsic membrane polypeptide gramicidin A in phospholipid bilayers. A solid-state carbon-13 nuclear magnetic resonance study. *Biophys. J.* 49:117-118.
- Takeuchi, H., Y. Nemoto, and I. Harada. 1990. Environments and conformations of tryptophan side chains of gramicidin A in phospholipid bilayers studied by Raman spectroscopy. *Biochemistry.* 29:1572-1579.
- Urry, D. W. 1971. The gramicidin A transmembrane channel: a proposed  $\pi(L,D)$  helix. *Proc. Natl. Acad. Sci. USA.* 68:672-676.
- Vogt, T. C. B., J. A. Killian, B. A. de Kruijff, and O. S. 1992. Influence of acylation on the channel characteristics of gramicidin A. *Biochemistry.* 31:7320-7324.
- Williams, L. P., E. J. Narcessian, O. S. Andersen, G. R. Waller, M. J. Taylor, J. P. Lazenby, J. F. Hinton, and R. E. Koeppe, II. 1992. Molecular and channel-forming characteristics of gramicidin K's: a family of naturally occurring acylated gramicidins. *Biochemistry.* 31:7311-7319.